COMITATO NAZIONALE PER L'ENERGIA NUCLEARE
Laboratori Nazionali di Frascati

LNF-72/42
18 Maggio 1972

G. Barbarino, F. Ceradini, M. Grilli, E. Iarocci, M. Nigro, R. Paoluzi, R. Santonico, P. Spillantini, L. Trasatti, V. Valente, R. Visentin and G. T. Zorn: EVALUATION OF PHOTON-PHOTON ANNIHILATION CONTRIBUTIONS IN A WIDE ANGLE EXPERIMENT AT ADONE.

Servizio Documentazione
dei Laboratori Nazionali di Frascati del CNEN
Casella Postale 70 - Frascati (Roma)

Laboratori Nazionali di Frascati del CNEN
Servizio Documentazione

LNF-72/42
18 Maggio 1972

G. Barbarino, F. Ceradini, M. Grilli, E. Iarocci, M. Nigro, R. Paoluzi, R. Santonico, P. Spillantini, L. Trasatti, V. Valente, R. Visentin and G. T. Zorn: EVALUATION OF PHOTON-PHOTON ANNIHILATION CONTRIBUTIONS IN A WIDE ANGLE EXPERIMENT AT ADONE. -

1. - Many authors[1] have pointed out that processes such as:

(1) $$e^+e^- = e^+e^- A\bar{A} \qquad (A \equiv e, \mu, \pi)$$

(2) $$e^+e^- = e^+e^- A\bar{A}A\bar{A}$$

occur within the present energy range for single beams of Adone, $E_+ = E_- = 700 - 1200$ MeV, and with cross sections which are "sizable" when compared with the common one-photon exchange process:

(3) $$e^+e^- = A\bar{A}$$

The same is also true if cross sections of processes (1) or (2) are compared with that of multihadron production (see ref. (2)), i.e. of process

(4) $$e^+e^- \longrightarrow n\pi^\pm + m\pi^o \quad \begin{pmatrix} n \geq 1, & m \geq 0 \\ n = 1 & m \geq 1 \end{pmatrix}$$

It is well known that processes (1) and (2) can be interpreted as due to the emission of a quasi-real photon by each incoming electron, followed

by a photon-photon annihilation with the creation of an $A\bar{A}$ pair (or an $A\bar{A}+A\bar{A}$ double pair). In the discussion which follows processes (1) and (2) will be referred to as "$\gamma\gamma$ processes" and processes (3) and (4) will be called a "one-photon processes"

Due to the fact that the cross sections for $\gamma\gamma$ processes increase logarithmically with energy, lnE, while those for the one photon exchange vary inversely with the square of the energy, E^{-2}, the contributions due to $\gamma\gamma$ processes are expected to increase in relative importance at the higher e^+e^- energies of future storage rings (CEA, Novosibirsk, DORIS, SPEAR, etc.).

In this paper events observed in the experimental arrangement of the our group at Adone are analysed in a search for those that could come from $\gamma\gamma$ processes, mainly in order to evaluate possible contaminations due to this mechanism to the one-photon processes. In the following we will test the reliability of this evaluation by comparing at a given total energy ($2E_{CM} \sim 2$ GeV), the expected and measured number of events due to $\gamma\gamma$ process. After this test the contaminations at different energies have been calculated, see Appendix II.

A drawing of one view of the apparatus is shown in Fig. 1. The trigger logic used in the seach for $\gamma\gamma$ processes is also indicated. A detailed description of the apparatus can be found in Reference 2.

The Monte-Carlo program used to estimate the efficiencies of the apparatus for the one photon processes(+) has been modified to calculate the efficiency for $\gamma\gamma$ processes, $\varepsilon_{TRIGGER}$, and to integrate their differential cross sections in order to obtain the total cross sections σ_{tot}. These, along with the effective cross sections that result from them, σ_{eff}, are listed in Table I for several center-of-mass energies ($E_{CM} = E_+ + E_-$). A description of the calculations appears in the Appendix I.

It is noteworthly the fact that, due the severe cuts introduced by our wide angle apparatus in the angular or energy distributions of produced $\gamma\gamma$ processes events (see one example in Fig. 3), σ_{eff} results to be strongly lower (by many order of magnitude) than σ_{tot}.

Photon-photon annihilation events which are most likely to be detected are those with two charged secondaries appearing as two tracks in the spark chambers of the apparatus. In that secondary electrons in these processes predominantly are emitted at small angles relative to the beam directions, the registered tracks will be close to coplanar

---

(+) - This Monte-Carlo program has been extensively used to determine the efficiencies of the apparatus of Fig. 1. It is described in Ref. (2).

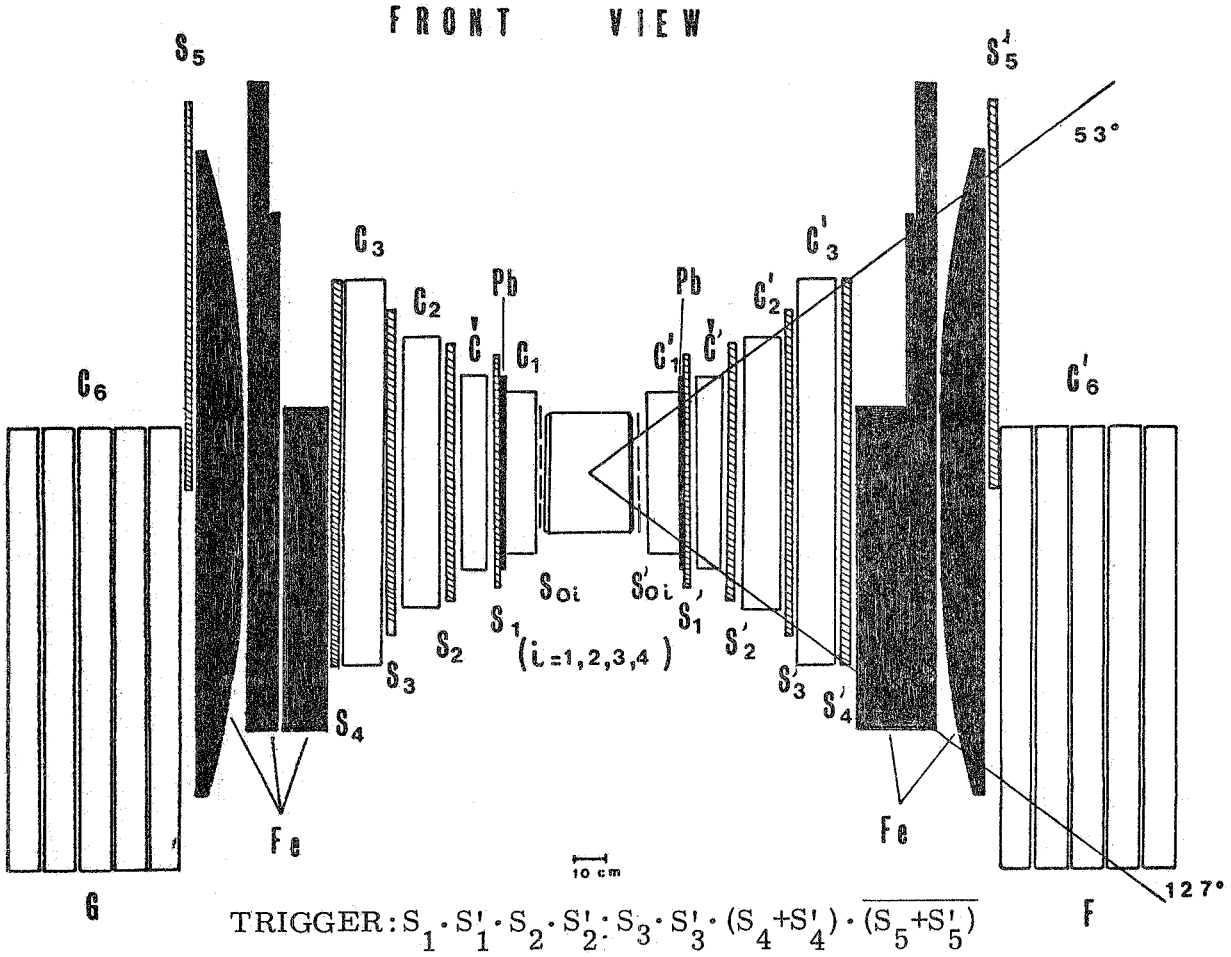

FIG. 1 - View of the main apparatus along the beam direction. C_1 (C'_1) are thin foil spark chambers used for space reconstruction of the events produced at the source, S, where the e^+e^- bunches collide. $C_2, C_3 \ldots$ (C'_2, $C'_3 \ldots$) are thick plate spark chambers used to observe the development of electromagnetic shower and/or the stop of charged particles. $S_o \div S_5$ ($S'_o \div S'_5$) are scintillation counters and $\check{C}$($\check{C}'$) are H_2O Cerenkov counter. The trigger logic used is also indicated.

TABLE I

Process	E_{CM} (GeV)	σ_{tot} ($10^{-33}cm^2$)	$\varepsilon_{trigger}$ (10^{-3})	σ_{eff} ($10^{-35}cm^2$)
A) $e^+e^- \rightarrow e^+e^- \mu^+\mu^-$	1.4 2.0 3.0	12 $\pm$.1 18.7$\pm$ 2 29 $\pm$ 3	3.8 $\pm$.4 3.9 $\pm$.4 3.2 $\pm$.3	4.55$\pm$.5 7.3 $\pm$.7 9.3 $\pm$.9
B) $e^+e^- \rightarrow e^+e^-\pi^+\pi^-$	1.4 2.0 3.0	.75$\pm$.08 1.37$\pm$.1 2.2 $\pm$.2	1.35$\pm$.1 2.4 $\pm$.2 1.7 $\pm$.2	.10$\pm$.01 .33$\pm$.03 .37$\pm$.04
C) $e^+e^- \rightarrow e^+e^-e^+e^-$	2.0	(7.3$\pm$0.7)10^6	(5.7$\pm$1)10^{-6}	4.2$\pm$1.0

with the beam but non-collinear(x). Thus, viewed along the beam direction, the tracks in the first spark chambers will form an angle of non coplanarity, $\Delta\phi$, which is near zero, and viewed perpendicular to the beams they will form an angle of non-coplanarity, $\Delta\theta$, which is greater than zero.

Of the three processes indicated by A), B) and C) in Table I only the first two, in fact, are to be considered. The latter, C), although produced with a substantial cross section is not reliably distinguishable, in the present experimental arrangement, from $e^+e^- \rightarrow e^+e^-\gamma$ which has an effective cross section more than fifty times larger. These processes with only electrons is the final state have been suppressed by the requirements that neither secondary particle produce either electromagnetic showers in succeding spark chambers C_2 and C_3, or a pulse height in counters 2 and 3 greater than a particle having twice the minimum ionization. The events of processes A and B in general may not be distinguished from each other and, in this analysis, their sum will be considered.

(x) - Notice that in our calculations (App. I) we have effectively used the equivalent photon approximation, which gives events exactly coplanar. The validity of this approximation, for process B) in Table I, has been discussed by Brodsky et al.(1).

The events due to the processes $ee \to ee\mu\mu$ and $ee \to ee\pi\pi$ are not observed without considerable background. The contamination due to unidentified electrons from $ee \to eeee$ and $ee \to ee\gamma$ has been estimated to be $< 2\%$. In addition, the contribution from other processes resembling them also have been estimated. Table II gives the efficiencies and the total and effective cross sections for processes D), $ee \to \varrho\gamma$ (Ref. 3), and E), $ee \to \mu\mu\gamma$ (Ref. 4), for various center-of-mass energies. The cross section for process E) integrated over the apparatus is seen to decrease rapidly with increasing energy E_{CM}. This results from the fact that events with muons having kinetic energies above ~ 600 MeV do not produce acceptable triggers and therefore are not considered if either muon traverses counter 5. In order to detect these events, a larger radiation energy loss is required as E_{CM} increases, but this results in an increasing large non-collinearity angle, $\Delta\theta$, which eventually reduces the effective solid angle for the apparatus to zero. Thus, in order to reduce the contamination due to process E), only data from runs at $E_{CM} > 1.8$ GeV were utilized in this study.

TABLE II

Process	E_{CM} (GeV)	σ_{tot} (10^{-33}cm^2)	$\varepsilon_{trigger}$ (10^{-3})	σ_{eff} (10^{-35}cm^2)
D) $e^+e^- \to \varrho^0\gamma$, $\varrho^0 \to \pi^+\pi^-$	1.4 2.0	5.6±.6 4.6±.5	2.5±.3 1.5±.2	1.4± .1 .7± .07
E) $e^+e^- \to \mu^+\mu^-\gamma$	1.4 1.5 1.8 2.0			45 ± 10 25 ± 5 1.4± .3 0

Additional background comes also from processe (4), quoted before, and from the process

F) $\quad e^{\pm}Z \to e^{\pm} + Z; \qquad e^{\pm}Z \to e^{\pm} + Z' + \pi$

Process (4) or multi-hadron production can result in two charged particles which trigger the apparatus and which lie within the angular interval of $\Delta\theta > 10^o$ and $\Delta\phi < 10^o$. Processes F) due to electron-nucleus

interaction on residual gas nuclei have been studied in separate experimental runs when events produced by single beams or spatially separated e^+e^- beams in Adone were detected. The predicted number of background events due to process F) within the selected angular intervals and having two non-electron-like secondaries was $\leq (3\pm2)\%$.

As indicated in the previous discussion, the rejection of events from process E) requires that only energies, E_{CM}, greater than 1.8 GeV be used. As the majority of the experimental observations above 1.8 GeV were made at 1.9 and 2.1 GeV, the analysis has been restricted to these energies.

In order to estimate the number of events due to processes A)+B), the observed two-track events have been analysed in the following way. The angular distribution in $\Delta\phi$ for events with two charged particles appearing in the apparatus (in opposite telescopes) was determined by selecting those events with $\Delta\theta > 10^o$. Due to the geometry of the apparatus and for beams which are unpolarized, this distribution in $\Delta\phi$ should follow a straight line. This has been demonstrated by Monte-Carlo calculations for multi-hadron events, processes F). The resulting experimental frequency distribution for $\Delta\phi$ along with a best-fit straight line based on events with $\Delta\phi > 10^o$ is shown in Fig. 2. The observed number of events appearing above the extrapolated best-fit line for $\Delta\phi < 10^o$ is 11 ± 6.7. For the purposes of normalization, it is noted that these events were observed contemporarily with 5527 $e^+e^- \rightarrow$ $\rightarrow e^+e^-$ or Bhabha scattering events.

The predicted number of events due to $\gamma\gamma$ processes A) and B) that should have been observed in this experimental sample with the time integrated luminosity of 1.33×10^{35} cm^{-2} is 9 ± 1. The predicted number of events within $\Delta\phi < 10^o$ and $\Delta\theta > 10^o$ due to processes D) and E) is 1 and due to process F) is $\leq (2\pm1)$. Thus the number of events due to $\gamma\gamma$ processes (A)+(B) (Table I) is consisted with that predicted by the theoretical calculations[1]. This result clearly is not statistically significant and is presented only as a status report on the analysis being carried out by this group at Adone. Moreover these results have been used to evaluate the contamination due to events coming from $\gamma\gamma$ processes on the multihadronic 2C-events (see Appendix II). Tagging at least one of the forward going electrons will certainly improve the signal to noise ratio and will permit more quantative observations to be made on these processes[5].

Data on events observed with tagging is now being collected by the $\mu\pi$ and $\gamma\gamma$ groups and will be published in the near future.

A preliminary paper also has recently been published on tagged events by $\gamma\gamma$ group [6].

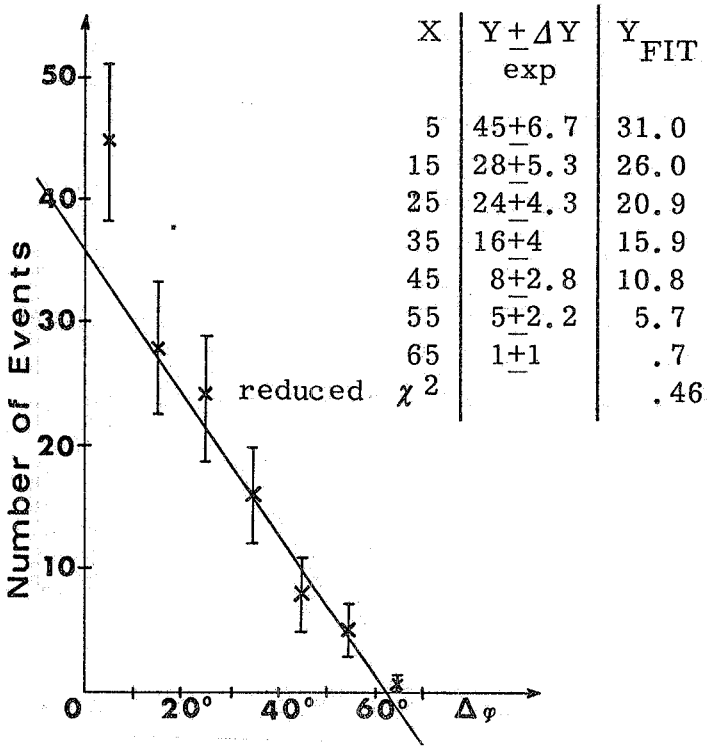

X	$Y \pm \Delta Y$ exp	Y_{FIT}
5	45±6.7	31.0
15	28±5.3	26.0
25	24±4.3	20.9
35	16±4	15.9
45	8±2.8	10.8
55	5±2.2	5.7
65	1±1	.7
reduced χ^2		.46

$$\left[\frac{Y-Y_{FIT}}{\Delta Y}\right]_{X=5} = \frac{45-31.0}{6.7} = \frac{14}{6.7} = 2.1\sigma$$

FIG. 2 - Experimental frequency distribution for $\Delta\varphi$. Included are events with only two visible charged--particle tracks.

APPENDIX I. -

A. 1. - $e^+e^- \longrightarrow e^+e^- \mu\mu(\pi\pi)$ effective cross sections. -

The effective cross section for processes

(1) $$e^+e^- \longrightarrow e^+e^- \mu^+ \mu^-$$

(2) $$e^+e^- \longrightarrow e^+e^- \pi^+ \pi^-$$

in a description based on equivalent real photons approximation is given by[1]:

$$\sigma_{eff} = \left(\frac{2\alpha}{\pi}\right)^2 \left[1g\left(\frac{E}{\mu}\right)\right]^2 \int_{4\mu^2}^{4E^2} \int_{s/4E^2}^{4E^2/s} \int_{-1}^{+1} P_1(s,\gamma) P_2(s,\gamma) x$$

(1.3)

$$x \left(\frac{d\sigma}{d(\cos\theta)}\right)_{\gamma\gamma} \eta(s,\gamma,\theta) \frac{ds}{s} \frac{d\gamma}{\gamma} d(\cos\theta)$$

where μ is the mass of the muon (pion), θ is the production angle in the C.M. system for $\mu\mu(\pi\pi)$ pairs in the reaction $\gamma + \gamma \longrightarrow \mu\mu(\pi\pi)$, s is the square of the four-momentum in the γ - γ system, $\gamma = 1+\beta_c/1-\beta_c$, β_c is the velocity of the center-of-mass of the γ - γ system, E is the energy of each incoming electron, $x_o = s/4E^2$, $P_1(s,\gamma) = 1/2(2-2\sqrt{\gamma x_o}+\gamma x_o)$, and $P_2(s,\gamma) = 1/2\,(2-2\sqrt{x_o/\gamma}+x_o/\gamma)$. The differential cross section for $\gamma\gamma \longrightarrow \mu\mu$ is:

(1.4) $$\left(\frac{d\sigma}{d\cos\theta}\right)_{\gamma\gamma} = 2\pi\alpha^2 \frac{\beta}{s} \left\{ \frac{1-\beta^4\cos^4\theta + \frac{8\mu^2}{s}\beta^2\sin^2\theta}{(1-\beta^2\cos^2\theta)^2} \right\}$$

and for $\gamma\gamma \longrightarrow \pi\pi$ is:

$$\left(\frac{d\sigma}{d\cos\theta}\right)_{\gamma\gamma} = \frac{\pi\alpha^2}{8} \frac{\beta}{s} \left\{ 16 + \frac{8}{D_1}\left[\frac{s}{2} - 4\mu^2 + s(1-\beta x)\right] + \right.$$

(1.5)

$$\left. + \frac{2}{D_1^2}\left[16\mu^4 - 8\mu^2 s(1-\beta x) + s^2(1-\beta x)^2\right] - \frac{4}{s}(s-4\mu^2)^2 \frac{1}{D_1} \right\}$$

where β is the velocity of the muon (pion) in the center-of-mass of the $\gamma\gamma$ system, $D_1 = -s/2(1-\beta x)$, $x = \cos\theta$, and $\eta(s, \gamma, \theta)$ is the detection efficiency for the experimental apparatus. The integration has been done by means of a Monte-Carlo calculation over the variables s, θ, and γ. Nuclear interactions of pions also were taken into account. The effective cross sections have been calculated by defining the function η as follows: $\eta = 0$ if an event with its particular values for s, γ, θ, is not accepted by the apparatus; $\eta = 1$ if it is accepted, i.e. results in a "good" trigger. To calculate the total cross sections η has been taken to be one. The resulting frequency distributions in the process A) for s, x, β_c and E_μ are shown in Fig. 3a, 3b, 3c and 3d. Separate distributions are shown for all events as well as for those detected by the apparatus.

The same formulas (1.3) and (1.4) have been used to calculate the integrated cross section for process $e^+e^- \longrightarrow e^+e^-e^+e^-$. An additional factor 1/4 has to be added to take into account the undistinguishibility of the incoming electrons after the bremsstrahlung, from those produced by the annihilation process $\gamma\gamma \longrightarrow e^+e^-$. To define the function η in this case we have used the probability for an electron to trigger the apparatus as a function of its energy. These probabilities have been estimated from measurements at various electron energies carried out at the Frascati Electrosynchrotron(x).

A.2. - $e^+e^- \longrightarrow \varrho^o\gamma$ effective cross section. -

Consider the following process:

(2.1)
$$e^+e^- \longrightarrow \varrho^o\gamma \qquad \varrho^o \longrightarrow \pi^+\pi^-$$

where the photon is produced in a bremsstrahlung process by one of the incoming electrons and the ϱ^o meson is created by annihilation of this electron, e', with the other electron,

(2.2)
$$e' + e \longrightarrow \varrho \, .$$

Assuming an equivalent real-photon distribution, the effective cross section for process (2.1) may be written as(4):

(2.3)
$$\sigma_{eff} = \frac{3}{16E} \int_{s_1}^{s_2} \int_{-1}^{+1} P(K)\,\sigma_V(s)\,(\sin^2\theta)\,\eta(s,\theta)\,\frac{ds}{K}\,d\cos\theta$$

(x) - These results have been reported and discussed in ref. (2).

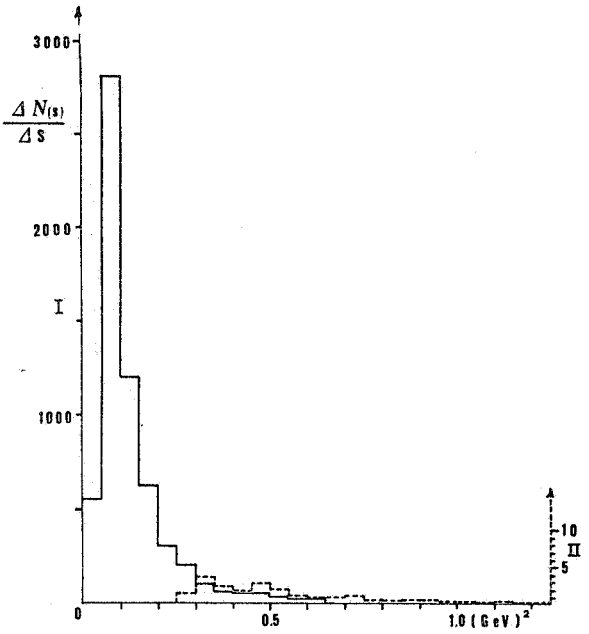

FIG. 3a) - Number of $e^+e^- = e^+e^- \mu^+ \mu^-$ events. vs s = (total energy in $\gamma\gamma$ CM system)^2.
Continuous line: all events. Broken line: events accepted by the apparatus.

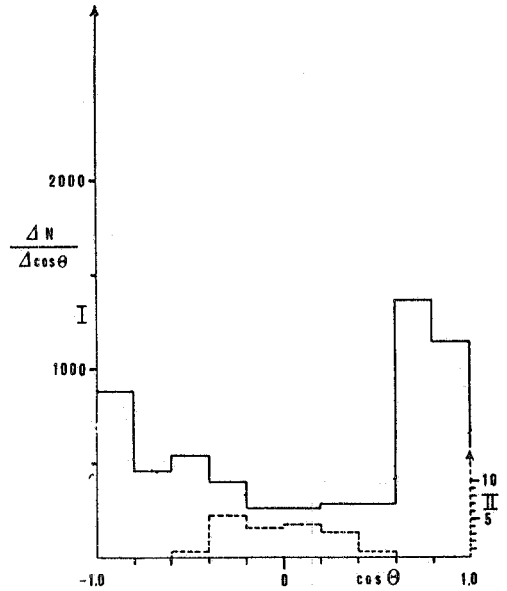

FIG. 3b) - Number of events vs cosθ where θ = production angle in $\gamma\gamma$ CM system.
Continuous line: all events. Broken line: events accepted by the apparatus.

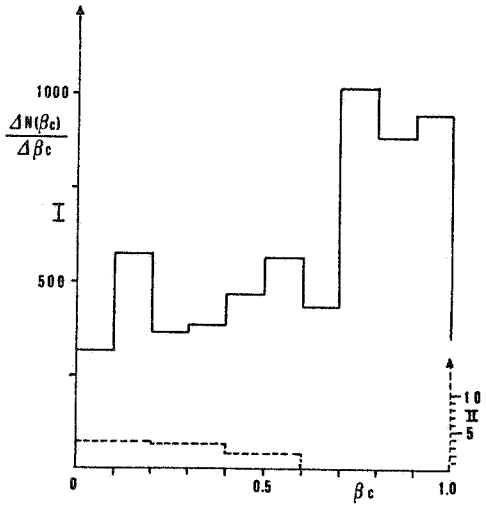

FIG. 3c) - Number of events vs β_c, velocity of the $\gamma\gamma$ CM system.
Continuous line: all events. Broken line: events accepted by the apparatus.

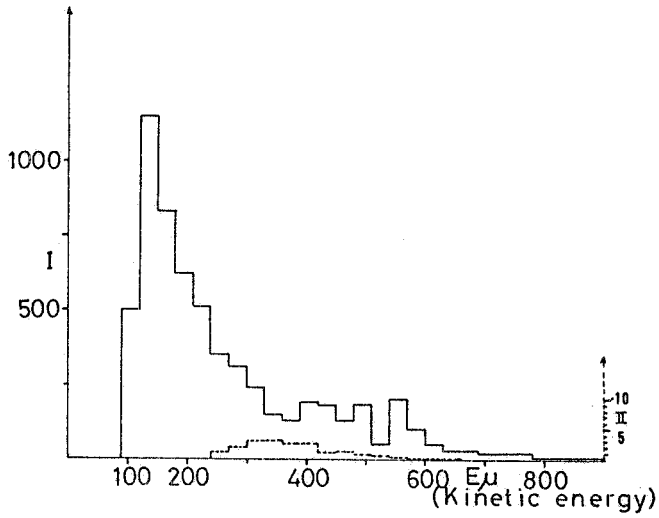

FIG. 3d) - Energy distribution of produced muons, from $e^+e^- = e^+e^- \mu^+ \mu^-$; E_μ = total energy of each μ in the LAB system.
Continuous line: all events (Scale I).
Broken line: events accepted by the apparatus (Scale II).

where s is the square of the four-momentum of the ϱ^o, E is the energy of the incoming electron, $K = (E - s/4E)$ is the energy of the radiated photon, θ is the angle of decay of the $\pi\pi$ pair in the reference system in which the ϱ^o is at rest, $P(K) = (4\alpha/\pi)\left[(E^2+(E-K)^2)/(2E^2)\right]\log(E/m)$, a factor depending on the photon energy distribution, $\sigma_V(s)$ is the total cross section for process (2.2) and $\eta(s,\theta)$ is a function describing the experimental apparatus efficiency. The term $(3/4 \sin^2\theta)$ takes into account the angular distribution of the pion pair in the ϱ center-of-mass system.

For $\sigma_V(s)$, a Breit-Wigner formula for the ϱ^o, with a peak at $s = m_\varrho^2 = 0.55\ GeV^2$ has been assumed. These may be written as follows:

$$\sigma_V(s) = \sigma_V(m_\varrho^2)\,\frac{m_\varrho^2\,\Gamma_\varrho^2}{(s-m_\varrho^2)^2 + m_\varrho^2\,\Gamma_\varrho^2}$$

and

$$\sigma_V(m_\varrho^2) = \frac{12\pi}{m_\varrho^2}\,\frac{\Gamma(\varrho \to ee)}{\Gamma_\varrho} = \frac{4\pi\alpha^2}{m_\varrho \Gamma_\varrho}\,\left(\frac{4\pi}{g_\varrho^2}\right),$$

where Γ_ϱ is the total $\varrho \to \pi\pi$ width and $g_\varrho^2/4\pi = 2.0 \pm 0.1$. The integration over s in (2.3) was taken from $s_1 = 0.16\ GeV^2$ to $s_2 = 1.2\ GeV^2$. The integration was performed by the same method described in (A.1), in which $\eta(s,\theta)$ was defined as a function which takes into account the geometry of the apparatus and the range and nuclear interactions of pions in it.

APPENDIX II. - Contamination from $\gamma\gamma$ processes on hadronic production events. -

In order to evaluate the cross section for multihadronic production, process (4), from the 2C-events (see Ref. 2), (i.e. events in which only two non collinear tracks, $\Delta\theta > 10^o$, have been detected) the events due to processes A) to E) must be regarded as background events and thus must be subtracted. As it has been said previously, the events from these processes are mostly coplanar, i.e. most of the two tracks appear with $\Delta\varphi \leq 10^o$ in the front view of the apparatus.

In the Table III are summarized the numbers of events for quoted processes, predicted by means of the calculations reported in the present work.

The corresponding total numbers of 2C-events are 33, 42 and 83, respectively (see Ref. 2).

TABLE III

2E (GeV)	Integrated luminosity $10^{33}cm^{-2}$	N° of events				
		$e^+e^-=e^+e^-\mu^+\mu^-$	$e^+e^-=e^+e^-\pi^+\pi^-$	$e^+e^-=\rho^o\gamma$	$e^+e^-=\mu^+\mu^-\gamma$	Total
1.5	29.8	1±.1	$\ll 1$	.3	4± 1	5± 1
1.9	43.5	3±.3	$\ll 1$	.3	.5	3±.4
2.1	90	7±.7	.3	.6	0	8± 1

Moreover, from the calculations carried out on reactions A) and B), contamination from these processes to the collinear (within 10^o) events due to two body hadronic process $e^+e^- = \pi^+\pi^-$ has also been estimated.

This contamination is $\sim$2% for $2E_{CM} = 1.4$ and $\sim$ 20% for 2E = = 2 GeV. We recall that all these calculations have been made in the equivalent photon approximation (see footnote (x) of pag. 4).

Details concerning the contaminations in two body hadronic process will be reported in a paper in preparation.

REFERENCES. -

See for instance:

(1) - M. Greco, Frascati report, LNF-71/1 (1971); S. G. Brodsky, T. Kinoshita and H. Terazawa, Cornell report CLNS-152 (1971).

(2) - G. Barbarino, F. Ceradini, M. Conversi, M. Grilli, E. Iarocci, M. Nigro, L. Paoluzi, R. Santonico, P. Spillantini, L. Trasatti, V. Valente, R. Visentin and G. T. Zorn, Frascati Report LNF-72/43 (1971); submitted to Nuovo Cimento.

(3) - C. Bernardini, Internal Report, INFN/AE-71/2 (1971).

(4) - G. Barbarino; Thesis of Rome University (1971) unpublished.

(5) - G. Barbiellini and S. Orito, Frascati Report LNF-71/17 (1971).

(6) - C. Bacci, G. Penso, G. Salvini, R. Baldini-Celio, G. Capon, C. Mencuccini, G. P. Murtas, A. Reale, M. Spinetti and B. Stella, Lett. Nuovo Cimento 3, 709 (1972).